ADVANCED FUNCTIONAL MATERIALS

www.afm-journal.de

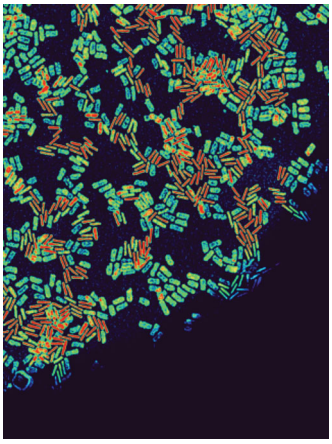

LEDs

In the search for better-performing colloidal light-emitting diodes (LEDs), nanocrystals of anisotropic morphologies remain to be explored. On page 295, Z. Chen et al. present the first functional LEDs based on quasi-2D core/shell CdSe/CdZnS nanoplatelets, where quantum confinement takes place in the direction of thickness. These solution-processed hybrid LEDs exhibit extremely narrow electroluminescence under different driving voltages, which is highly promising to achieve superior color purity.

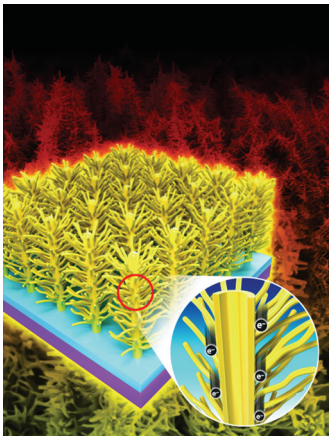

Dye-Sensitized Solar Cells

J. H. Kim and co-workers present a facile and effective method to prepare hierarchical pine tree-like TiO_2 nanotube arrays with an anatase phase directly grown onto a transparent conducting oxide substrate via a one-step hydrothermal reaction. On page 379, the length of the nanotube arrays is increased by up to 19 μm to significantly improve the specific surface area and charge transport in dye-sensitized solar cells.

Microstructures

Fibroblasts are shown here pulling on a protein micropillar array. On page 277, B. P. Chan et al. show such complex protein microstructures and micropatterns can be fabricated using multiphoton-based free-writing, via the expression of specific adhesion molecules. This protein micropillar array presents a simple "write-and-seed" platform for cell niche studies.

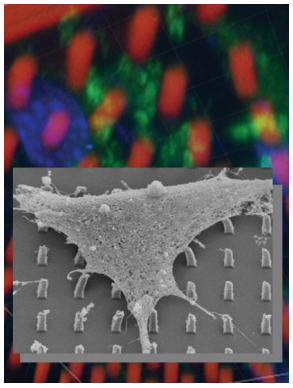

CONTENTS

FULL PAPERS

Microstructures

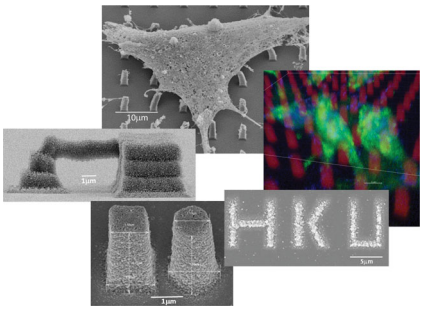

Multiphoton-based free-writing of 3D complex protein microstructures and micropatterns, with sub-micrometer features and controllability over voxel dimension, morphology, and porosity, is reported. Protein micropillar array presents a simple "write-and-seed" platform for cell niche studies. Fibroblasts attach to, grow on, express adhesion molecules and deposit extracellular matrices on these arrays without matrix coating.

LEDs

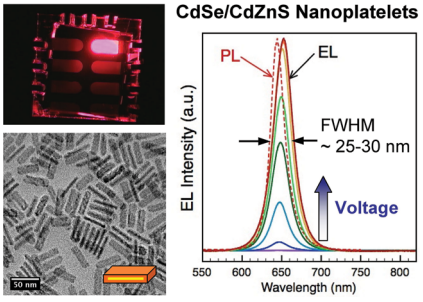

The first light-emitting diodes (LEDs) based on quasi-2D colloidal core/shell CdSe/CdZnS nanoplatelets (NPLs) under a solution-processed hybrid device structure are reported. Over different applied voltages, systematically narrow electroluminescence of FWHM in the range of 25–30 nm is observed, which is highly attractive in terms of color purity in the context of LED applications.

Water Splitting

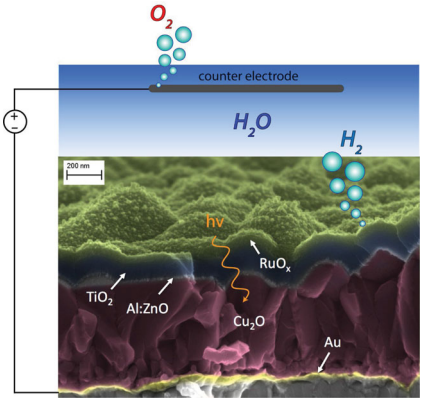

Ruthenium oxide on cuprous oxide photocathodes enhanced by a built-in p–n junction yields an active catalyst for hydrogen generation from water and unprecedented 94% stability over 8 h of light chopping chronoamperometry at 0 V vs. the reversible hydrogen electrode. The photocurrents obtained would correspond to greater than 6% solar-to-hydrogen efficiency in a tandem cell configuration.

Phase Transition

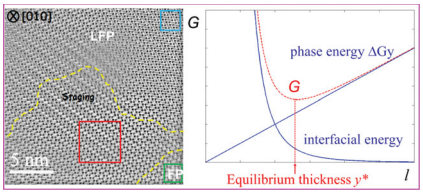

The phenomenon of Li-ordering in the system $LiFePO_4/FePO_4$ is investigated by STEM-ABF for different sizes. While in small crystals, the ordering affect the whole particle; for larger crystals, it was found to characterize the $LiFePO_4/FePO_4$ contact and the interfacial zones narrow with increasing size. These findings are discussed in the light of phase transition thermodynamics and kinetics.

FULL PAPERS

Robust composite structures consisting of Fe_3O_4 nanoparticles (~5 nm) embedded in uniform mesoporous carbon spheres with an average size of about 70 nm (IONP@mC) are synthesized with the purpose of application in high-rate batteries. Under high current densities ranging from 500 to 10 000 mA g^{-1}, such composites deliver stable and high reversible capacities, reaching 271 mAh g^{-1} at 10 000 mA g^{-1}.

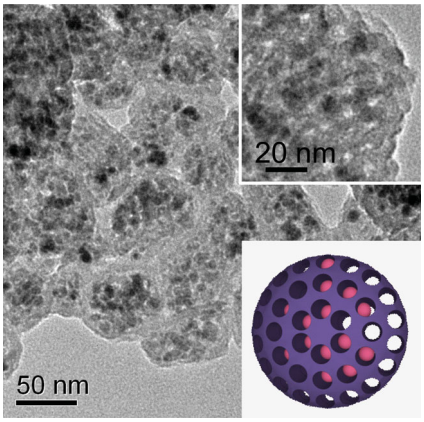

Batteries

A detailed investigation of the formation and properties of chiral nematic mesoporous silica (CNMS) templated by cellulose nanocrystals is presented. These materials are made by a simple self-assembly process and have tunable chirality, mesoporosity, and photonic properties. The chiral pore structure of these materials may provide unique opportunities for applications including refractometric sensing.

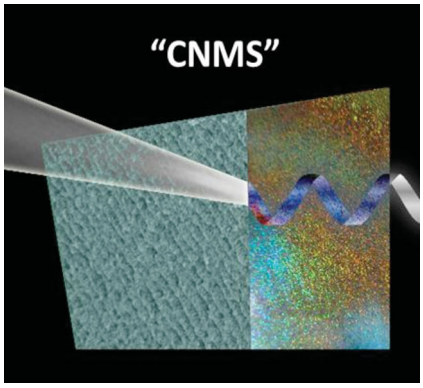

Self-Assembly

A model is developed to calculate the intersubband (blue arrow) and intrasubband (red arrows) photocurrents in an InAs/GaAs quantum dot solar cell. Temperature-dependent quantum efficiency measurements are reproduced with good agreement. The results reveal the radiative nature of the thermal escape from the quantum dots, and explain the difficulty in measuring intrasubband transitions.

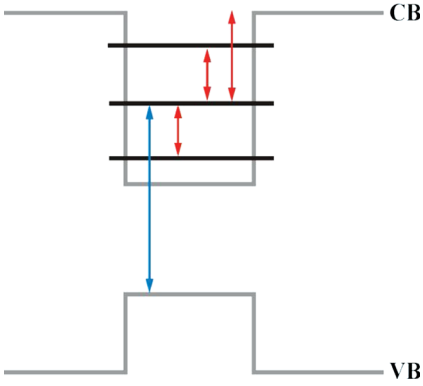

Solar Cells

Shape-adaptive, hyperbranched polyurea with quaternary ammonium compounds. The preparation of AB2 monomers and the covalently attached hyperbranched polyurea coatings with polyethyleneimine covalently coupled to hyperbranched polyurea coatings. The coatings demonstrate high contact-killing efficacies toward adhering staphylococci, without any demonstrable leaching of antibacterial compounds.

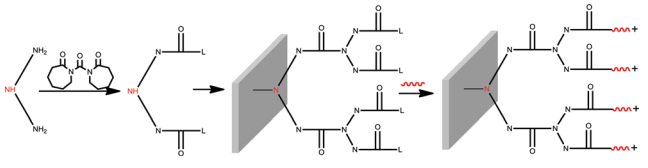

Antibacterials

CONTENTS

FULL PAPERS

Piezoceramics

Relaxor/Ferroelectric Composites: A Solution in the Quest for Practically Viable Lead-Free Incipient Piezoceramics

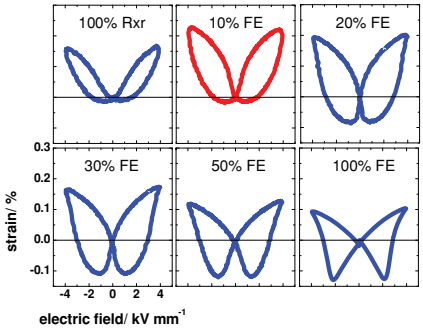

Incipient piezoceramics are featured by giant strain of ≈0.4%. However, this giant strain is only realized at relatively large electric field (>4 KV mm^{-1}) with a significant strain hysteresis. Here, many of the challenges the incipient piezoceramics face can be overcome by relaxor/ferroelectric composite approach.

Tumor Therapies

Near-Infrared Photoregulated Drug Release in Living Tumor Tissue via Yolk-Shell Upconversion Nanocages

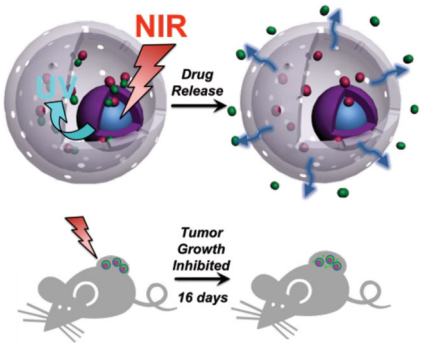

A near-infrared (NIR) phototrigger-controlled drug-release device (PDD) is designed using yolk-shell structured nanocages with upconversion nanophosphors as yolks and silica as shells (YSUCNP). The anticancer drug chlorambucil caged with a coumarin phototrigger is accommodated by YSUCNPs to a large loading capacity of 49 wt%. By employing NIR light with deep tissue penetration depth as stimuli, the PDD demonstrates efficacy in living tumor-bearing mice with zero premature release.

Hydrogen Production

Enhanced Hydrogen Production by Photoreforming of Renewable Oxygenates Through Nanostructured Fe_2O_3 Polymorphs

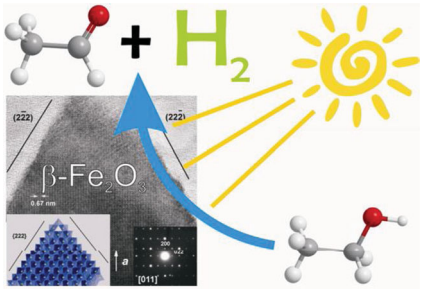

Sunlight-activated photoreforming of renewable oxygenates promoted by Fe_2O_3 nanosystems is a very attractive process for hydrogen production. In this context, scarcely investigated β- and ε-Fe_2O_3 polymorphs, fabricated by chemical vapor deposition, show very promising performances for photocatalytic solar hydrogen generation. The present approach holds a remarkable potential even for the synthesis of added-value by-products, paving the way to manifold technological applications.

Dye-Sensitized Solar Cells

High Efficiency Solid-State Dye-Sensitized Solar Cells Assembled with Hierarchical Anatase Pine Tree-like TiO_2 Nanotubes

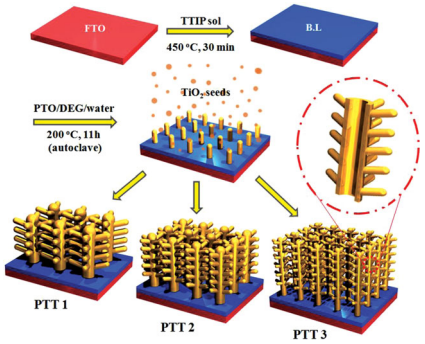

Hierarchical, 19 μm long, anatase, pine tree-like TiO_2 nanotube arrays directly grown on a transparent conducting oxide via a one-step hydrothermal reaction result in high-efficiency, solid-state dye-sensitized solar cells. The efficiency is 8.0% at 100 mW/cm^2, one of the highest values observed for the N719 dye.

FULL PAPERS

Saturated polar-substituted elastomers are obtained via functional-group tolerant catalytic insertion polymerization. This novel direct approach to hydrocarbon- and oil-resistant elastomers is compatible with a wide range of cross-linking chemistries, which results in useful mechanical and thermal properties as well as solvent-resistance.

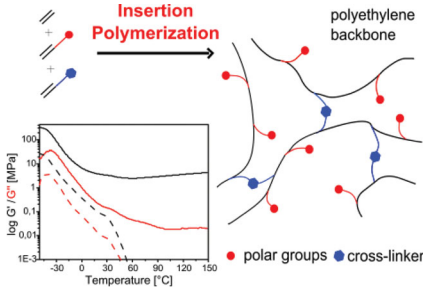

Elastomers

The mechanical response of monolayer graphene on polyethylene terephthalate is characterized using in-situ Raman spectroscopy and atomic force microscopy. Two interfacial failure mechanisms, shear sliding under tension and buckling under compression, are identified. The interfacial shear strength is found to range between 0.46 and 0.69 MPa. Beyond a critical compressive strain of around –0.7%, buckling ridges are observed.

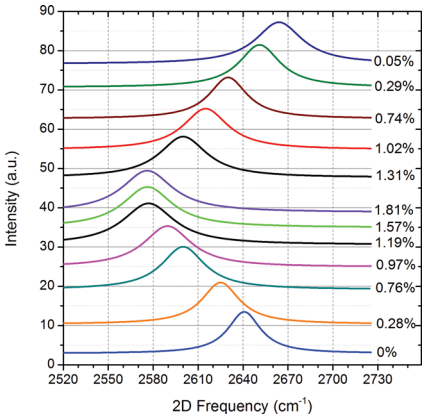

Graphene

Optically transparent antibacterial films capable of healing scratches to restore transparency are fabricated by incorporating triclosan into branched polyethylenimine/poly(acrylic acid) multilayer films. Sustained release of triclosan endows the films with antibacterial properties. Film transparency can be healed multiple times by immersing the films in water or spraying water on them.

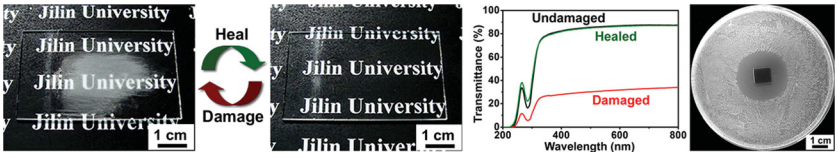

Self-Healing Materials